

SEASONAL AND INTER-ANNUAL VARIABILITY OF REMOTELY-SENSED SEA SURFACE HEIGHT, VISIBLE LIGHT AND CHLOROPHYLL IN THE BAY OF BENGAL

Dissertation Submitted for the partial fulfillment for the degree of

MASTER OF SCIENCE IN PHYSICS

By

Mithun M. Gawas & Anuj S. Pokle

Under the guidance of

Dr. S. Prasanna Kumar

Scientist 'F' (POD), NIO, Goa



Department of Physics
Goa University, Taleigao Plateau
April 2008

CERTIFICATE

This is to certify that the project entitled

SEASONAL AND INTER-ANNUAL VARIABILITY OF REMOTELY-SENSED
SEA SURFACE HEIGHT, VISIBLE LIGHT AND CHLOROPHYLL IN THE
BAY OF BENGAL

Submitted by

Mithun M. Gawas and Anuj S. Pokle

Dissertation submitted in partial fulfillment for the degree of

MASTER OF SCIENCE IN PHYSICS
GOA UNIVERSITY

Is record of their work carried out in N.I.O

Head of Department

Project Supervisor

Examiner

Date: 10th April 2008.

ACKNOWLEDGEMENT

Presenting this project report titled” Seasonal and inter-annual variability of remotely-sensed sea surface height, visible light and chlorophyll in the Bay of Bengal” gives us an immense pleasure. We specially thank the Director of NIO for allowing us to do the project in NIO And also Dr. Desa, Head, Department of Physics, Goa University for permitting us to do the same.

We express our sincere thanks to our guide Dr. S. Prasanna Kumar for providing us with his invaluable time, and ideas.

We would also like to thank Mr. Gourish Salgaonkar for his immense help during the course of this dissertation.

CONTENTS

Topic	Page- No
Chapter 1 INTRODUCTION 1.1 Introduction 1.2 Objectives of the study 1.3 Study Region – Bay of Bengal	1-6 1 4 5
Chapter 2 DATA AND METHODOLOGY 2.1 Introduction 2.2 The Concept 2.3 Principle of Remote Sensing 2.4 Remote Sensing Satellites 2.5 Parameters Used for Present Study	7-24 7 7 8 16 24
Chapter 3 RESULTS AND DISCUSSION 3.1 Sea Surface Height Anomaly 3.2 Chlorophyll a 3.3 Photosynthetically Available Radiation 3.4 Diffusion Attenuation	25-35 25 29 32 34
Chapter 4 SUMMARY	36-38
References	39

CHAPTER 1

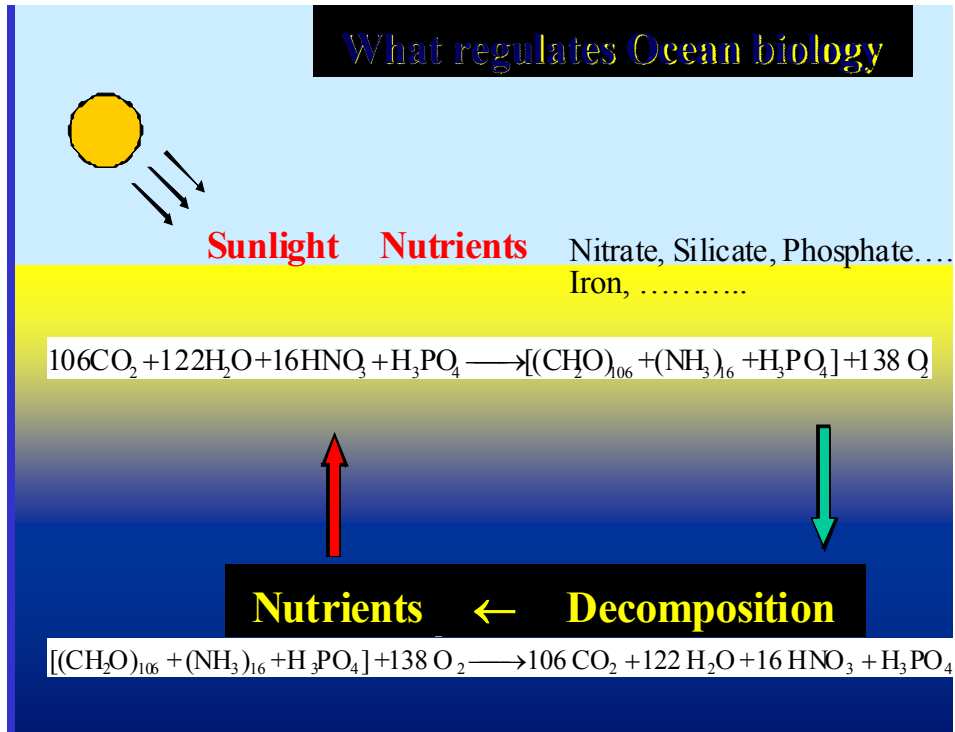
INTRODUCTION

1.1 Introduction

Earth-Ocean-Atmosphere as a whole is undergoing a change, which is unprecedented in the history of mankind and the available scientific data, suggests its link to the increased concentration of carbon dioxide. The burning of fossil fuel releases carbon dioxide to the atmosphere and being a green house gas it traps the solar radiation. This increase in the trapping efficiency of the solar radiation by the increasing concentration of carbon dioxide in turn increases the temperature of the earth-ocean-atmosphere system, which is known as a human-induced global warming. The human-induced global warming has several manifestations such as melting of glaciers and polar ice caps, increase in sea level, changing pattern of floods and droughts, etc. Along with change in the physical climate system the ecosystem, both terrestrial as well as aquatic, also are under stress. The global warming and climate change is one of the major threats faced by the mankind in the present century. For example, the sea-level rise will affect the large populations that are concentrated along the coastal region in addition to the large deltaic plains such as Sundarban region. The increased temperature and coastal flooding will increase the chances of outbreak of vector-borne diseases such as malaria, dengue etc. It is in this context that the study on global warming and climate change assumes importance. Ocean plays an important role in the climate of the earth as it covers 70.8% of the total earth surface and acts as a reservoir of carbon. In fact the

phytoplankton's, the tiny microscopic plants of the ocean, accounts for about 40% of the earth's total annual photosynthetic production. The phytoplankton takes up the inorganic carbon from the atmosphere as carbon dioxide and converts them into organic carbon with the help of sunlight and nutrients (nitrate, phosphate, silicate)

depicted
Figure



as
in the
1.

Figure 1 Schematic representation of photosynthetic process in the ocean by phytoplankton.

These phytoplankton are consumed by small zooplankton, which in turn is eaten by larger zooplankton and finally by the fish completing the marine food chain. Once the phytoplankton and the zooplankton die and decay (bacterial action) the organic carbon is converted back into inorganic CO₂ and released back to atmosphere. A part of the dead phytoplankton as well as the zooplankton and the fecal pellets of zooplankton will settle down to the ocean bottom. Thus, a part of the inorganic carbon from the atmosphere will be removed permanently to the ocean bottom. This is known as the ocean biological pump and is shown in Figure 2.

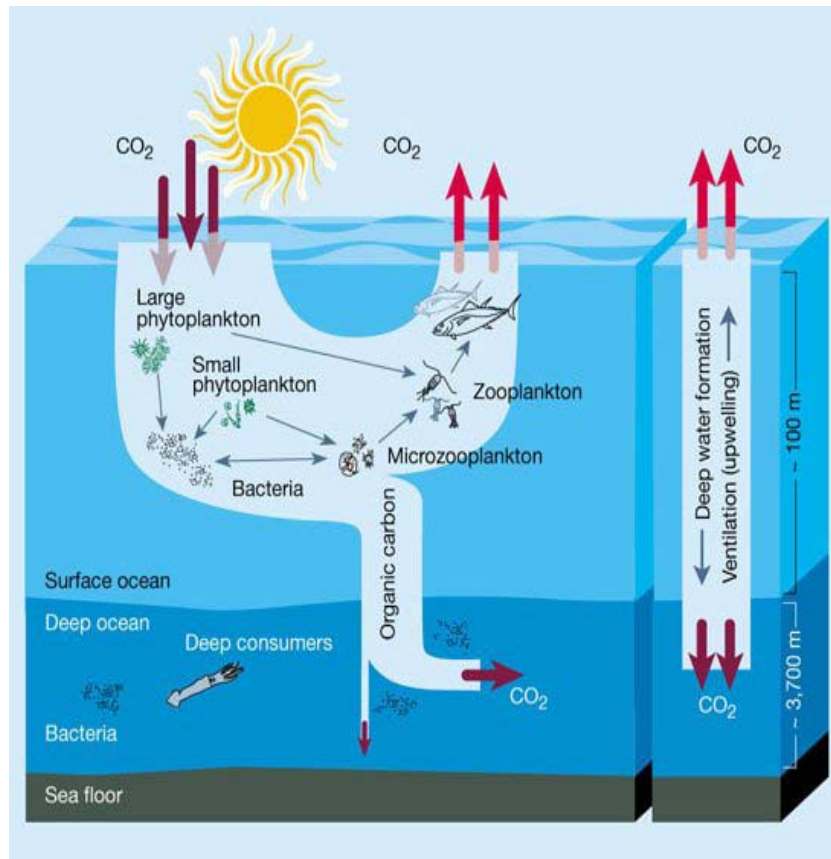
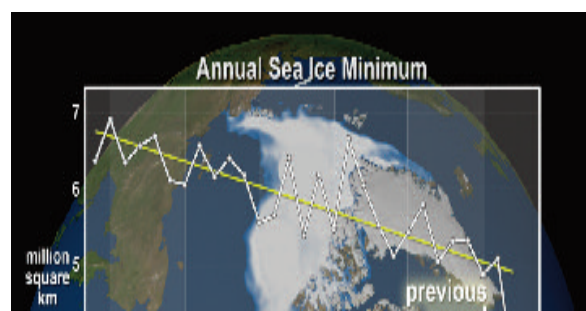
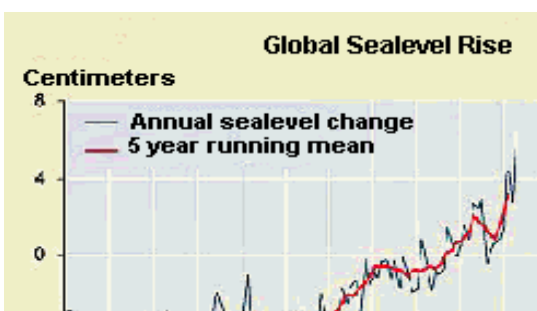


Figure 2 Schematic representation of ocean biological pump

Thus, phytoplankton forms the basis of ocean life and regulates CO_2 and O_2 levels in the atmosphere. Hence it is important to understand the phytoplankton biomass and its variability with time.

Another parameter useful for monitoring large-scale climate variability is the sea level. It integrates virtually all-static and dynamic processes in the hydro-sphere and atmosphere. A long-term increase in the Ocean's sea level (see Figure 3a) is an indication of global warming due to the melting of glaciers and polar ice-caps (see Figure 3b). Rising sea level and increase in storm activity, which is one of the scenarios predicted under global warming, will intensify coastal erosion and enhance coastal flooding.



a

b

Figure 3 (a) Global sea level rise during 1880-1980 (Source: <http://www.poemsinc.org/FAQ/sealevel.html>), and **(b)** declining Greenland ice-cover from 1979-2007 (source: National snow and ice data)

1.2 Objectives of the study

The objective of the present project work is to understand the long-term variability of phytoplankton biomass and sea level, which are the important two parameters for understanding the global climate change. This is accomplished by understanding the seasonal and inter-annual variability of

1. Chlorophyll pigment concentrations (Chl *a*)
2. Photosynthetically available radiation (PAR)
3. Diffuse attenuation coefficient (kd490)
4. Sea-surface height anomaly (SSH)

The phytoplankton biomass at any given location depends on the amount of sunlight available for photosynthesis and the nutrients. PAR indicates the amount of sunlight available at the surface of the ocean and kd490 tells us how deep this light will penetrate which in turn determines the depth within which phytoplankton can effectively carry out photosynthesis.

1.3 Study region – Bay of Bengal

The Bay of Bengal is a tropical basin situated in the western part of the north Indian Ocean (Figure 4). The Bay of Bengal is a unique basin, which is land, locked in the north and forced by semi-annually reversing monsoon winds. Northeast monsoon winds are weak and bring cool and dry continental air during

winter (November-February). But the southwest monsoon winds during summer are strong and bring humid maritime air. The surface waters of the Bay of Bengal is less saline (see Figure 4) and this happens due to large amount of oceanic precipitation which is about 2 m yr^{-1} (Prasad, 1997). Huge quantities of fresh water of about $1.625 \times 10^{12} \text{ m}^3 \text{ yr}^{-1}$ (Subramanian, 1993) from the major rivers such as Ganges-Brahmaputra, Mahanadi, Godavari, Krishna, Pennar and Irrawady also contribute in reducing the saltiness of the surface waters. In addition to the fresh water, these rivers also bring huge quantity of suspended sediment, estimated to be about 1.4×10^9 tonnes, to the Bay.

These sediments will influence the upper water column of the Bay of Bengal in two ways – (1) the sediments will bring some amount of nutrients along with them which will influence the biological productivity in terms of carbon fixation by phytoplankton, (2) the suspended sediments in the water column will influence the downward penetration of the visible light which is very essential for photosynthesis.

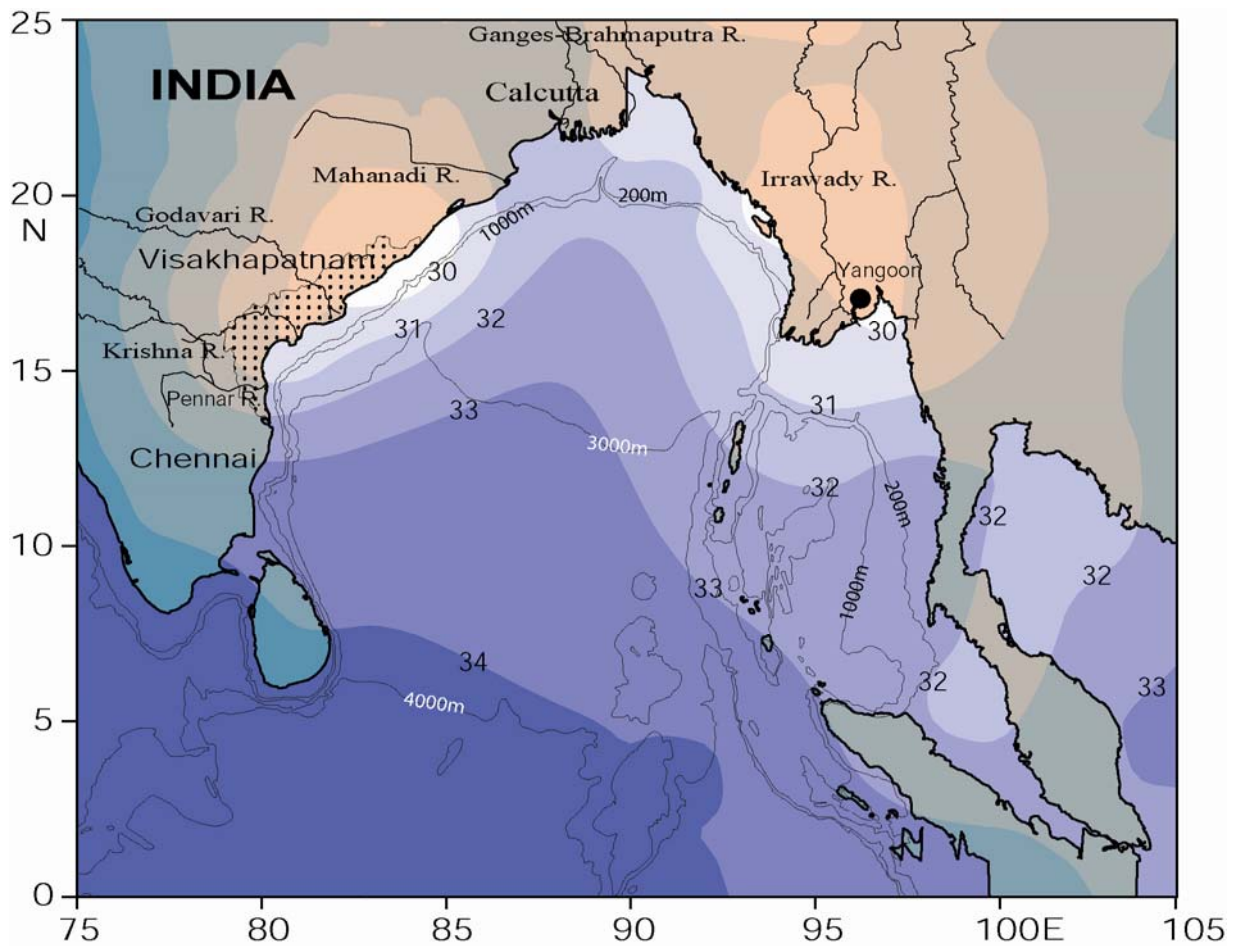


Figure 4 Location map of the Bay of Bengal. Rivers Ganges-Brahmaputra, Mahanadi, Godavari, Krishna, Pennar and Irrawady are also shown. The colour shading shows the distribution of annual mean salinity (psu). Salinity data was taken from Levitus et al., 1994. The depth contours (thin dark line) are in meters

CHAPTER 2

DATA AND METHODOLOGY

2.1 Introduction

It is very difficult, time consuming and expensive to conduct ground (in situ) and Aerial survey to gather information from a region as large as the Bay of Bengal. More over even if we manage to get a one-time such measurement of the parameters of interest, it will be virtually impossible to repeat such measurement over a long period of time to understand the spatial variability over seasonal, annual and interannual time scale. Hence the only alternative is to resort to remote sensing technique to gather the necessary information.

2.2 The Concept

Remote Sensing involves gathering data and information about the physical world by detecting and measuring signals composed of radiation, particles, and fields emanating from objects located beyond the immediate vicinity of the sensor device. So it's a rather simple, familiar activity that we all do as a matter of daily life, but that gets complicated when we increase the scale at which we observe. Several of the human senses gather their awareness of the external world almost entirely by perceiving a variety of signals, either emitted or reflected, actively or passively, from objects that transmit this information in waves or pulses. Thus, one hears disturbances in the atmosphere carried as sound waves, experiences sensations such as heat (through radiant energy) etc.

Specifically Remote Sensing is a technology for sampling electromagnetic radiation to acquire and interpret data from which to extract information about features, objects, and classes on the Earth's land surface, oceans, and atmosphere (also on the exteriors of other bodies in the solar system, or, in the broadest framework, celestial bodies such as stars and galaxies). Applied Remote Sensing involves the detecting and measuring of electromagnetic energy (usually photons) emanating from distant objects made of various materials, so that the user can identify and categorize these objects - usually, as rendered into images - by class or type, substance, and spatial distribution.

2.3 Principle of Remote Sensing

In order to understand the data that is obtained by remote sensing technique, it is important to understand the electromagnetic spectra, the energy radiated by objects, characteristics of digital image, etc.

Electromagnetic Radiation

The principle of remote sensing is simply that of measuring the varying energy levels of a single entity, the fundamental unit in the electromagnetic force field known as the photon. Photon energy is directly proportional to the frequency of the wave and inversely to its wavelength. The electromagnetic (EM) radiation that varies from high to low energy levels comprises the Electro Magnetic spectrum (EMS) (see Figure 5). Based on the wavelength, the electromagnetic spectrum can be divided into the following:

1. **Radio Waves:** 10 cm to 10 km.
2. **Microwaves:** 1 mm to 1 m.
3. **Infrared:** 0.7 to 300 μm .
4. **Visible Light:** 400 nm (violet) to about 700 nm (red).
5. **Ultraviolet:** 3 to 400 nm.
6. **X-Rays:** 10-.01 nm
7. **Gamma Rays:** below 10 Pico meter.

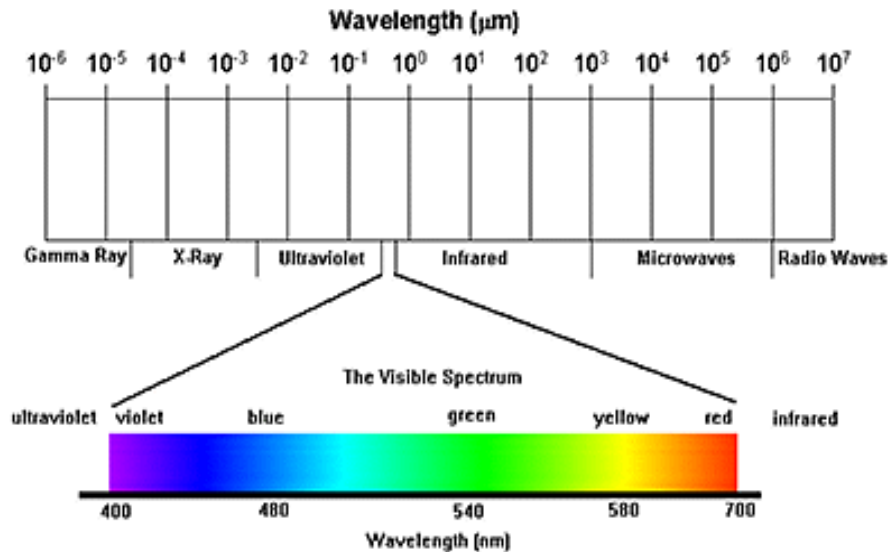


Figure 5 Electromagnetic spectrum from Radio waves to Gamma rays. The visible part is depicted in an expanded form. (Source: <http://www.crisp.nus.edu.sg/~research/tutorial/em.htm>)

As explained above, the electromagnetic spectrum can be divided into several wavelength (frequency) regions, among which only a narrow band from about 400 to 700 nm is visible to the human eyes (Figure 5). Note that there is no sharp boundary between these regions. The boundaries shown in the above figures are approximate and there are overlaps between two adjacent regions.

The photon is the physical form of a quantum, the basic particle studied in quantum mechanics (messenger particle for EM force). These particles also move as waves and hence, have a "dual" nature. These waves follow a pattern that can be described in terms of a sine (trigonometric) function as shown in Figure 6.

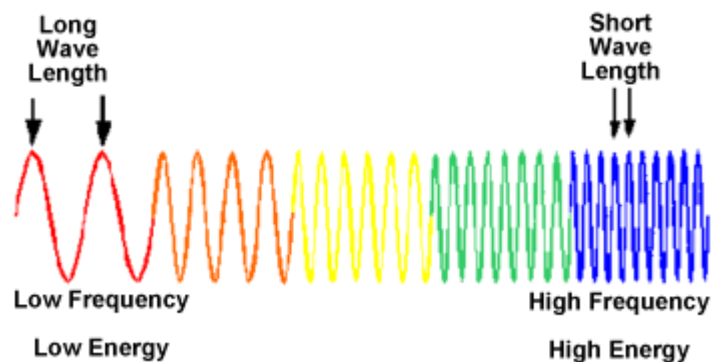


Figure 6 Schematic depicting the wave pattern of the photon having high and low frequency.

A photon is said to be quantized, in that any given one possesses a certain quantity of energy. Some other photon can have a different energy value. Photons as quanta thus show a wide range of discrete energies. The amount of energy characterizing a photon is determined using Planck's general equation:

$$\mathbf{E = h\nu}$$

Where h is Planck's constant ($6.6260... \times 10^{-34}$ Joules-sec)* and ν is the Greek letter, nu, representing frequency. Photons traveling at higher frequencies are therefore more energetic. If a material under excitation experiences a change in energy level from a higher-level E_2 to a lower level E_1 , we restate the above formula as:

$$\mathbf{\Delta E = E_2 - E_1 = h\nu}$$

Where ν has some discrete value determined by $(\nu_2 - \nu_1)$. In other words, a particular energy change is characterized by producing emitted radiation (photons) at a specific frequency ν and a corresponding wavelength at a value dependent on the magnitude of the change.

The frequency of the photon is determined by method known as the photoelectric effect. From a quantum standpoint, the maximum kinetic energy is given by

$$\mathbf{K.E. = h\nu + W \text{ (the energy needed to free the electron)}}$$

This equation indicates that the energy associated with the freed electron depends on the frequency (multiplied by the Planck constant h) of the photon that strikes the plate plus a threshold amount of energy required to release the electron (W , the work function). By measuring the current, and if that work energy is known and other adjustments are made, the frequency of the photon can be determined.

To measure the total energy radiated by any object, we use Stefan-Boltzmann Law which states that the total energy radiated per unit surface area of a black body in

unit time j^* , is directly proportional to the fourth power of the black body's thermodynamic temperature T

$$j^* = \sigma T^4$$

For a body that doesn't absorb or emit the full amount of radiation, a general equation is given as,

$$j^* = \epsilon \sigma T^4$$

Where ϵ emissivity of a material.

It is also important to know the property of the material. This is given by Beer-Lambert Law, which relates the absorption of light to the properties of the material through which the light is travelling. This law states that there is a logarithmic dependence between the transmissivity of light through a substance and the concentration of the substance and path length of material that the light travels through i.e.

$$T = I/I_0 = e^{-\alpha l}$$

Where α is the absorption coefficient and l is the distance that light travels through the material. Thus if α and l are known the concentration of a substance can be deduced from the amount of light transmitted by it.

After being familiar with relation between the light absorbed and the material property, there's another relation between the temperature and the wavelength of the body. This is seen from Wien's law (see Figure 7), which states that wavelength carrying the maximum energy is inversely proportional to the absolute temperature i.e. hotter the body, shorter, is the wavelength. It has the form,

$$\lambda_{\max} T = \text{constant}$$

Where λ_{\max} is the wavelength of maximum intensity and T is the temperature

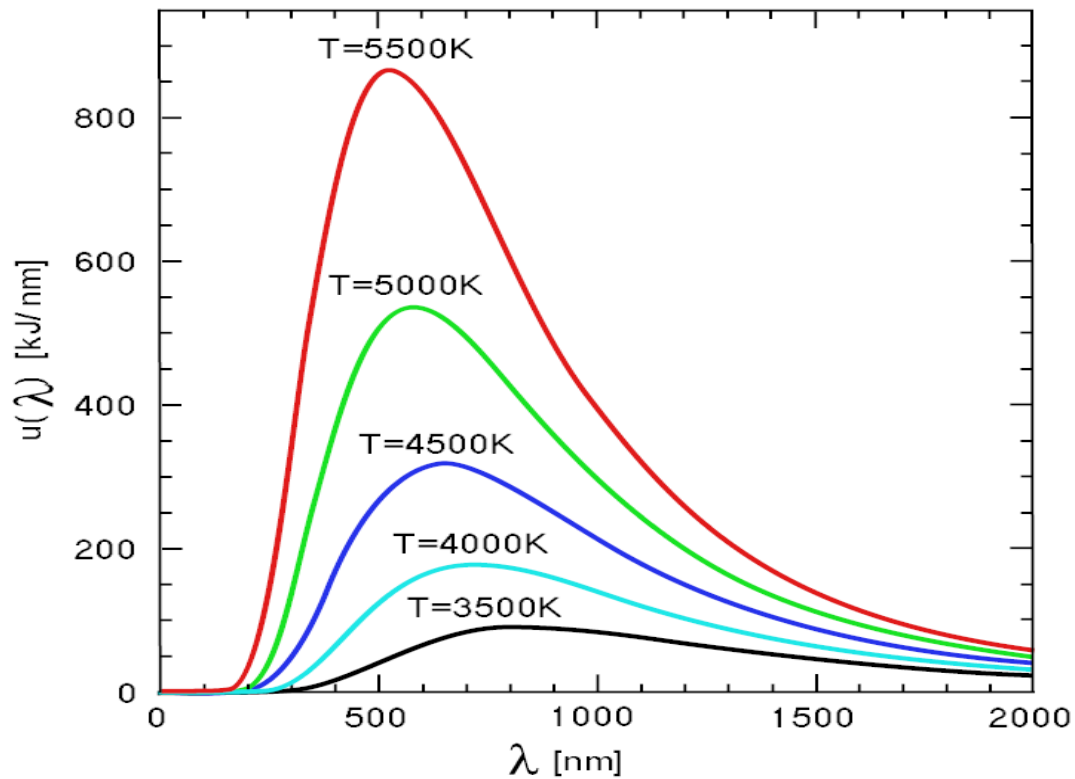


Figure 7 Graph representing Wien's Law
 (Source: http://en.wikipedia.org/wiki/Wien's_displacement_law)

Analog and Digital Images

An image is a two-dimensional representation of objects in a real scene. Remote sensing images are representations of parts of the earth surface as seen from space. The images may be analog or digital. Aerial Photographs are examples of analog images while satellite images acquired using electronic sensors are examples of digital images. A digital image is a two-dimensional array of pixels. Each pixel (see Figure 8) has an intensity value (represented by a digital number) and a location address (referenced by its row and column numbers).

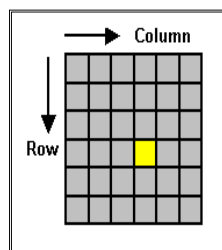


Figure 8 Schematic representation of a Pixel

Pixels

A digital image comprises of a two dimensional array of individual picture elements called pixels arranged in columns and rows. Each pixel represents an area on the Earth's surface. A pixel has an intensity value and a location address in the two dimensional image.

The intensity value represents the measured physical quantity such as the solar radiance in a given wavelength band reflected from the ground, emitted infrared radiation or backscattered radar intensity. This value is normally the average value for the whole ground area covered by the pixel.

The intensity of a pixel is digitized and recorded as a digital number. Due to the finite storage capacity, a digital number is stored with a finite number of bits (binary digits). The number of bits determines the radiometric resolution of the image. For example, an 8-bit digital number ranges from 0 to 255 (i.e. $2^8 - 1$), while a 11-bit digital number ranges from 0 to 2047. The detected intensity value needs to be scaled and quantized to fit within this range of value. In a Radiometrically calibrated image, the actual intensity value can be derived from the pixel digital number.

The address of a pixel is denoted by its row and column coordinates in the two-dimensional image. There is a one-to-one correspondence between the column-row address of a pixel and the geographical coordinates (e.g. Longitude, latitude) of the imaged location. In order to be useful, the exact geographical location of each pixel on the ground must be derivable from its row and column indices, given the imaging geometry and the satellite orbit parameters.

Spatial Resolution

Spatial resolution refers to the size of the smallest object that can be resolved on the ground. In a digital image, the resolution is limited by the pixel size, i.e. the

smallest resolvable object cannot be smaller than the pixel size. The intrinsic resolution of an imaging system is determined primarily by the instantaneous field of view (IFOV) of the sensor, which is a measure of the ground area viewed by a single detector element in a given instant in time. However this intrinsic resolution can often be degraded by other factors, which introduce blurring of the image, such as improper focusing, atmospheric scattering and target motion. The pixel size is determined by the sampling distance.

A High Resolution image refers to one with a small resolution size. Fine details can be seen in a high-resolution image. On the other hand, a Low Resolution image is one with a large resolution size, i.e. only coarse features can be observed in the image. The image resolution and pixel size are often used interchangeably. In reality, they are not equivalent. An image sampled at a small pixel size does not necessarily have a high resolution.

Radiometric Resolution

Radiometric Resolution refers to the smallest change in intensity level that can be detected by the sensing system. The intrinsic radiometric resolution of a sensing system depends on the signal to noise ratio of the detector. In a digital image, the radiometric resolution is limited by the number of discrete quantization levels used to digitize the continuous intensity value.

Having described the technique of remote sensing it is also important to understand about the type of remote sensing satellite, the sensors used and the parameters it can measure.

2.4 Remote Sensing Satellite

Satellite imaging system

Several remote sensing satellites are currently available, providing imagery suitable for various types of applications. Each of these satellite-sensor platforms is characterized by the wavelength bands employed in image acquisition, spatial resolution of the sensor, the coverage area and the temporal coverage.

In terms of the spatial resolution, the satellite imaging systems can be classified into:

- Low resolution systems (approx. 1 km or more)
- Medium resolution systems (approx. 100 m to 1 km)
- High resolution systems (approx. 5 m to 100 m)
- Very high resolution systems (approx. 5 m or less)

In terms of the spectral regions used in data acquisition, the satellite imaging systems can be classified into:

- Visible and Reflective Infrared Remote Sensing
- Thermal Infrared Remote Sensing
- Microwave Remote Sensing

Optical/thermal imaging systems can be classified according to the number of spectral bands used:

- Monospectral or panchromatic (single wavelength band, "black-and-white", grey-scale image) systems
- Multispectral (several spectral bands) systems
- Superspectral (tens of spectral bands) systems
- Hyperspectral (hundreds of spectral bands) systems

Synthetic aperture radar imaging systems can be classified by the combination of frequency bands and polarization modes used in data acquisition, e.g.:

- Single frequency (L-band, or C-band, or X-band)

- Multiple frequencies (Combination of two or more frequency bands)
- Single polarization (VV, or HH, or HV)
- Multiple polarizations (Combination of two or more polarization modes)

Satellite Orbits

A satellite follows a generally elliptical orbit around the earth. The time taken to complete one revolution of the orbit is called the orbital period. The satellite traces out a path on the earth surface, called its ground track, as it moves across the sky. As the earth below is rotating, the satellite traces out a different path on the ground in each subsequent cycle. Generally there are two types of orbits that are used for the study of ocean-atmosphere-earth system and they are the polar orbiting and the geosynchronous orbit (Figure 9).

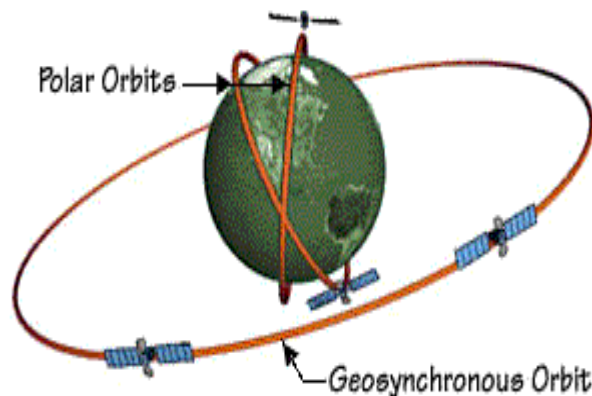


Figure 9 Orbit of a polar orbiting satellite and geosynchronous satellite
(Source:<http://daac.gsfc.nasa.gov/atmosphere/dynamics/documentation/remote.sml>)

Geosynchronous satellites are used for communication and meteorological application such as tracking of weather systems; cyclones etc. while Polar orbiting satellites are generally used for remote sensing application in the study of ocean, earth and atmosphere to study the spatio-temporal variability. Remote sensing satellites are often launched into special orbits such that the satellite repeats its path after a fixed time interval. This time interval is called the repeat cycle of the

satellite. Usually remote sensing satellites orbit at a distance of about 700-900Km from the surface of the earth.

In the present project work we have used the satellite altimetry to obtain the sea level data while optical remote sensing (visible light) for obtaining the information on phytoplankton chlorophyll, diffuse attenuation coefficient and photosynthetically available radiation, it is important to give a brief description about them.

Satellite altimetry

Altimetry is a technique for measuring height which falls under microwave remote sensing. Satellite altimetry measures the time taken by a radar pulse to travel from the satellite antenna to the surface and back to the satellite receiver. Combined with precise satellite location data, altimetry measurements yield sea-surface heights.

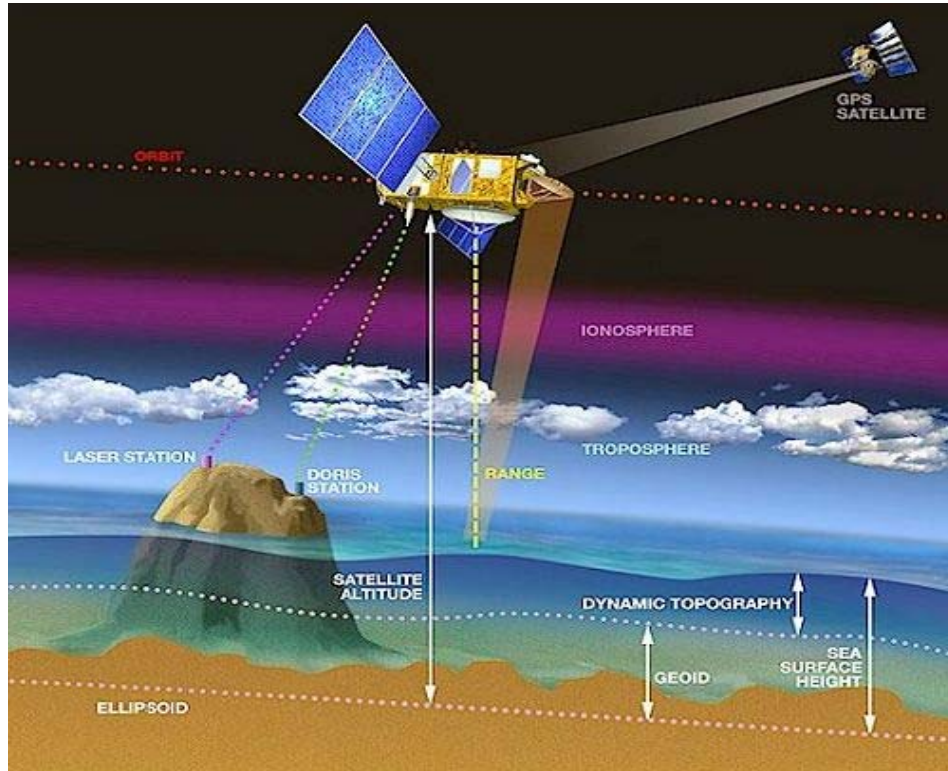


Figure 10 Working of Satellite Altimetry
(Source: www.avisioceanobs.com/en/altimeter)

There's a simple principle underlying this technique (see Figure 10) wherein altimeters emit signals to Earth, and receive the echo from the sea surface, after its reflection. Radar altimeters on board the satellite permanently transmit signals at high frequency (over 1700 pulses per second) to Earth, and receive the echo from the sea surface. This is analyzed to derive a precise measurement of the round-trip time between the satellite and the sea surface. The time measurement, scaled by the speed of light (at which electromagnetic waves travel), yields a range measurement. By averaging the estimates over a second, this produces a very accurate measurement.

There are specific bands of frequencies which are used in altimetry (see Figure 11)

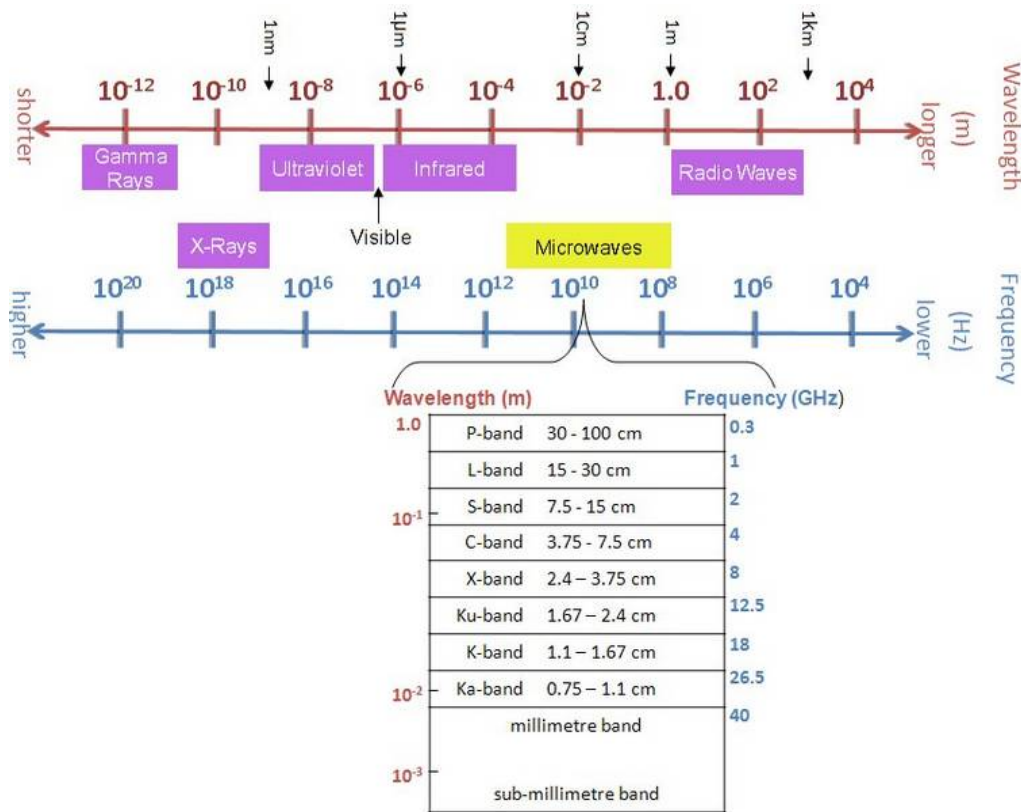


Figure 11 Extended view of the frequency bands useful in satellite altimeter
(Source: www.aviso.oceanobs.com/en/altimeter)

From the above figure K_u band is the most commonly used frequency. It is the best compromise between the capabilities of the technology (relating to power emitted), the available bandwidth (determined by international regulations for specific

applications), sensitivity to atmospheric perturbations, and perturbation by ionospheric electrons.

Ocean Color

Unlike satellite altimetry ocean color deals with optical remote sensing. The color of the ocean is determined by the interactions of incident light with substances or particles present in the water. Ocean is blue due to the absorption and scattering of light. The blue wavelengths of light are scattered, similar to the scattering of blue light in the sky but absorption is a much larger factor than scattering for the clear ocean water. In water, absorption is strong in the red and weak in the blue, thus red light is absorbed quickly in the ocean leaving blue. Important substances which influence the color of the ocean are phytoplankton, suspended material, yellow substances (group of organic, dissolved substances, consisting of humic and fulvic acids), and the bottom effect (applicable in shallow waters).

From the above mentioned criteria's the most important light-absorbing substance in the ocean are the free-floating photosynthetic organisms (phytoplankton) and inorganic particulates. Phytoplankton contains chlorophyll, which absorbs light at blue and red wavelengths and transmits in the green. Particulate matter can reflect and absorb light, which reduces the clarity (light transmission) of the water. Substances dissolved in water can also affect its color. By studying the color of the light scattered from the oceans, optical sensors can quantify the amount of chlorophyll and other constituents.

Light upwelling from the sea surface after back-scattering in water carries useful information on the water body. The atmospheric contributions and specular reflection at the sea surface constitute noise in this context, and have to be corrected for. At the altitude of a satellite sensor, more than 80% of the light reaching the detector may have an atmospheric origin (Morel, 1980), and small errors in estimating the atmospheric contribution can cause significant biases in the

estimation of the water component. Furthermore, the upwelling component from the water has to be processed to evaluate what the water-leaving component would have been, if there were no atmosphere in between the sensor and the water body.

The Factors that influence upwelling light, leaving the sea surface are

- (i) Upward scattering by inorganic suspended material
- (ii) Upward scattering from water molecules
- (iii) Absorption by the yellow substances component
- (iv) Reflection off the bottom
- (v) Upward scattering from the phytoplankton component

Note that absorption by any of these components or by the bottom will serve to decrease the water-leaving signal. Light from the sun may be scattered by atmospheric constituents before it reaches the sea surface. Similarly, light leaving the water may be scattered away from, or towards the remote sensor by the atmosphere (see Figure 12)

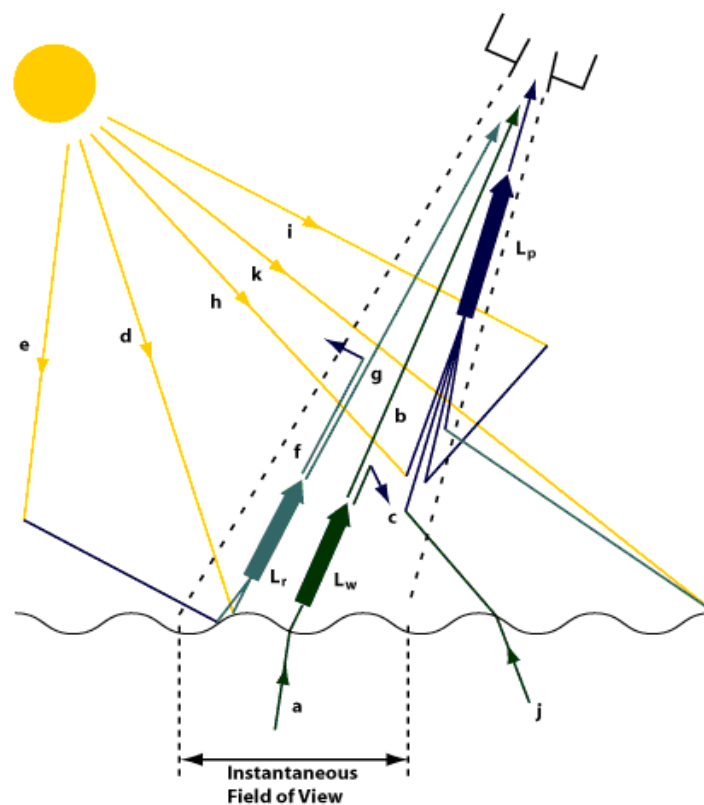


Figure 12 Scattering of light while travelling through the atmosphere as well as in water.

From the optical point of view oceanic waters are classified into Case 1 and Case 2 waters. Where

- **Case 1:** represent the phytoplankton-dominant water
- **Case 2:** represent all other possible cases including suspended material, yellow substances etc.

This classification implies that all the optical properties of Case 1 waters can be modelled as a function of chlorophyll *a* concentration.

2.5 Parameters Used for the Present Study

In this project work basically we deal with 4 parameters such as sea surface height (SSH), Chlorophyll *a* (Chl-*a*), Photosynthetically Available Radiation (PAR), Diffusion Attenuation (kd490).

The monthly gridded SSH anomaly data was obtained from Topex/Poseidon satellite altimeter. (<http://apdrc.soest.hawaii.edu/las/servlets/dataset?catitem=1000>). SSH data was from January 1992 to December 2006. Topex/Poseidon allows estimation of the global average sea level to a precision of several millimeters in 10 days. It is nadir pointing radar altimeter using C band (5.3 GHz) and Ku band (13.6 GHz) for measuring sea surface height.

The rest of the 3 parameters (Chl-*a*, PAR, kd490) were obtained from SeaWiFs (Sea-viewing Wide Field-of-view Sensor) ocean color data (<http://oceancolor.gsfc.nasa.gov/>). The monthly mean data was from September

1997 to September 2007. The satellite on which it flies (Orb View-2) has a swath of 2801Km; resolution is 1.1Km and 8 bands.

Software which were used to view and analyze the data were Seadas and Ferret for interpreting data into an image and to obtain the plots respectively, whereas Matlab was used for curve fitting.

CHAPTER 3

RESULTS AND DISCUSSION

To decipher the seasonal variability, the monthly mean climatology was computed for all the 4 parameters.

3.1 Sea Surface Height Anomaly

Seasonal variability

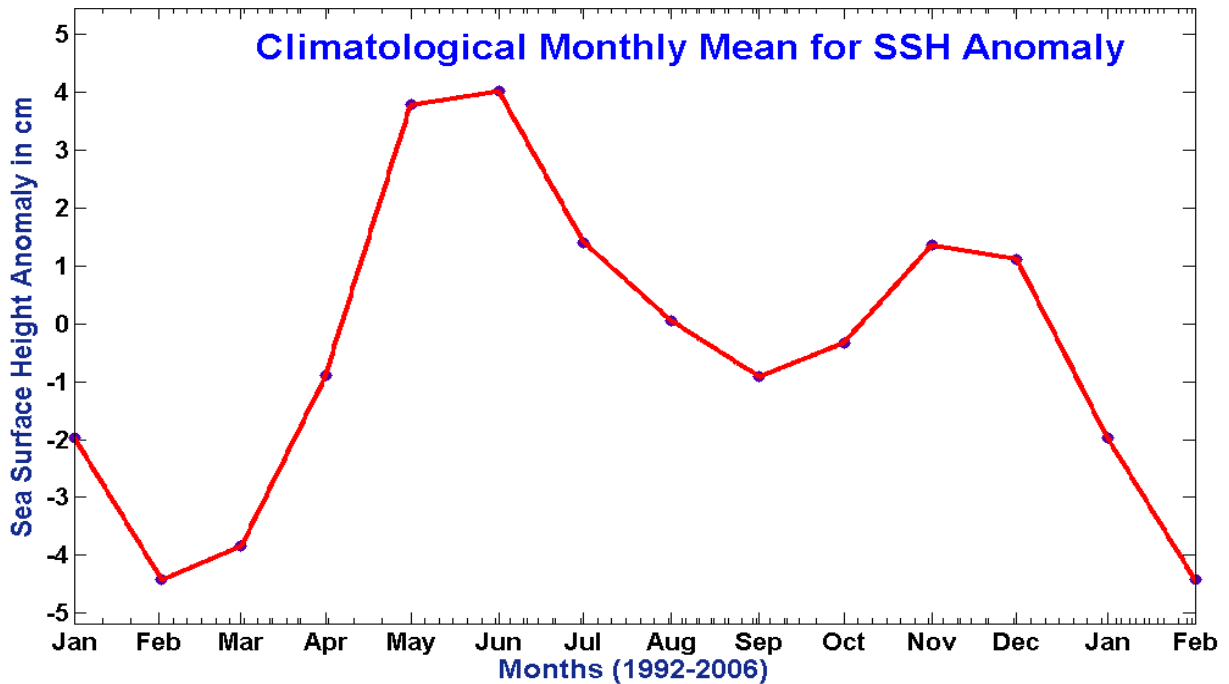


Figure 13 Monthly mean climatology of SSH anomaly

The monthly mean climatology of SSH (Figure 13) showed a bi-modal distribution with highest SSH anomaly occurring in May-June (4cm) followed by a secondary peak in November-December (~2cm). Similarly the lowest SSH anomaly occurred in February followed by the 2nd lowest in September.

Inter-annual variability

In order to understand the inter-annual variability, the entire data set was analyzed (Figure 14)

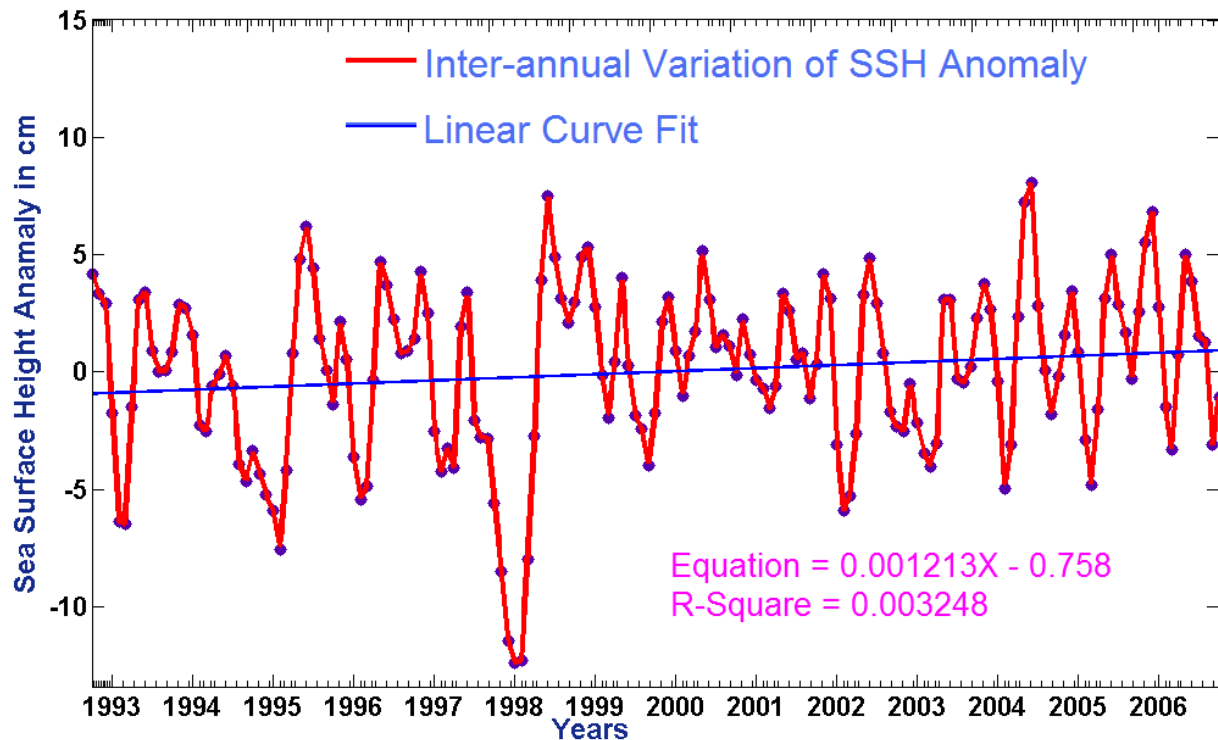


Figure 14 Monthly mean of SSH anomaly during 1992 to 2007

The SSH anomaly curve showed large variability from -13cm to +8cm (Figure 14). The linear trend line (solid blue line) showed an increasing trend over the period of study. That is the sea level showed an increase with time from 1992 to 2007 of about ~2cm. As the SSH showed large seasonal variability, it is important to know which are the months that contributed towards this increasing trend. For this we further analyzed SSH anomaly for the 4 months namely February, May, September and November were selected as these were the months which showed the maximum and minimum anomaly.

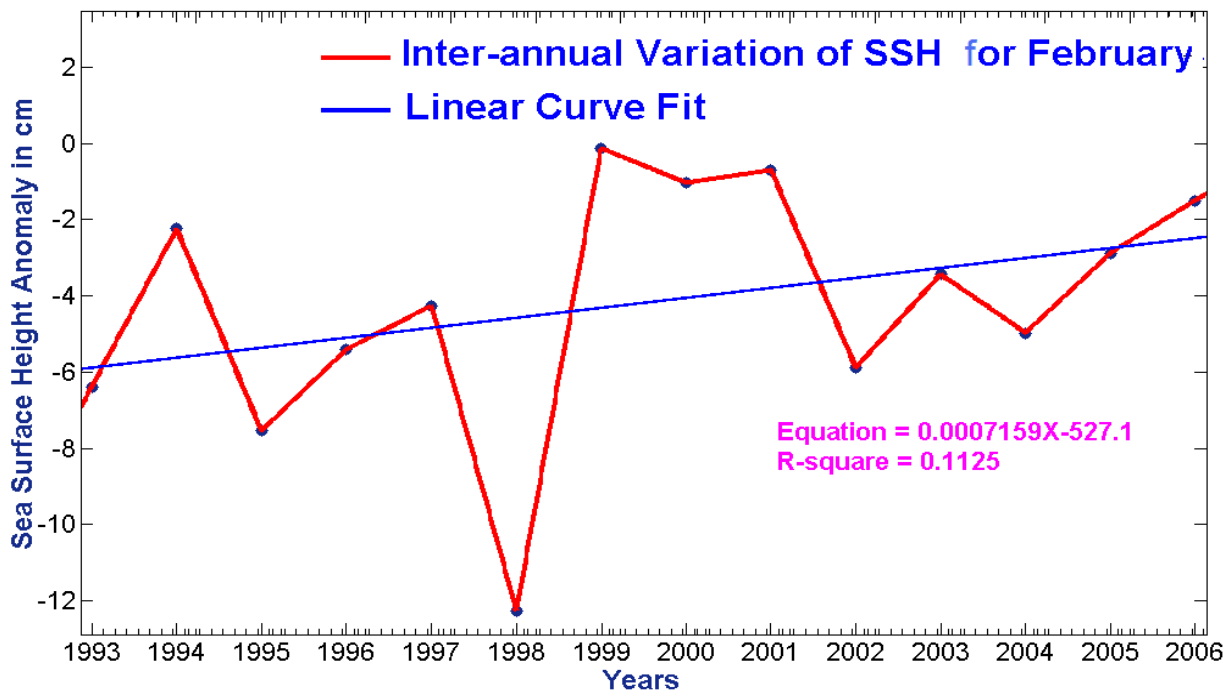


Figure 15 Monthly mean of SSH anomaly for February

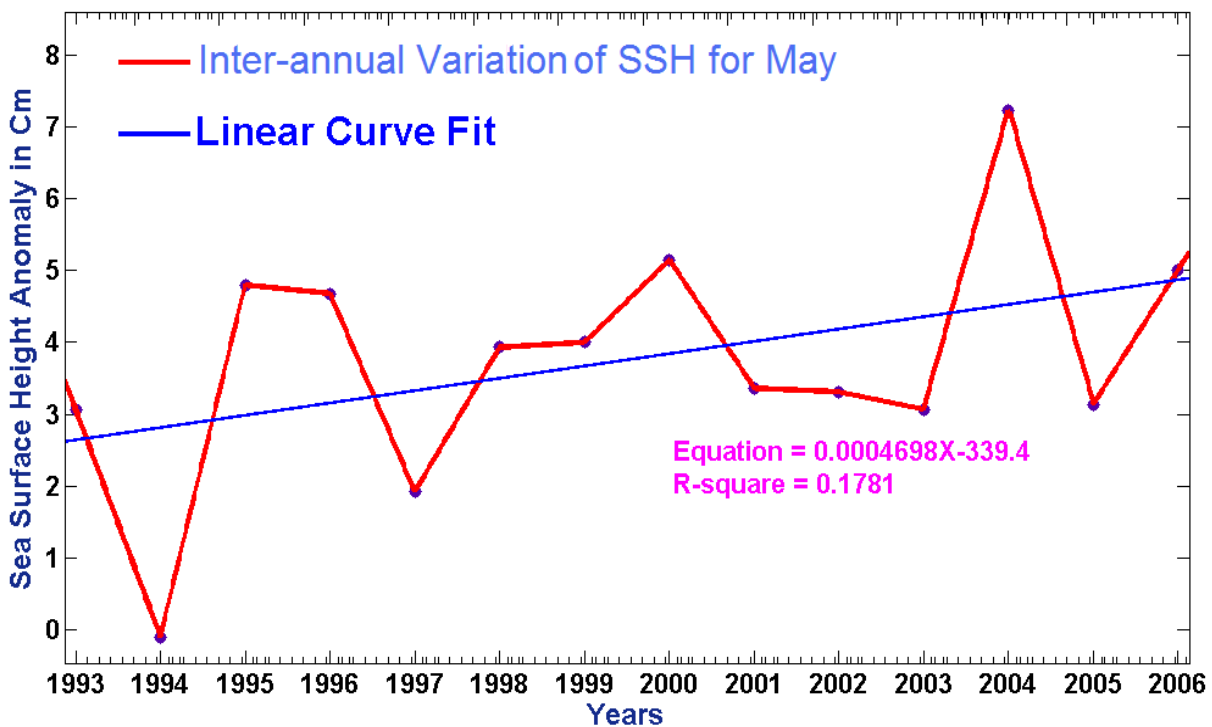


Figure 16 Monthly mean of SSH anomaly for May

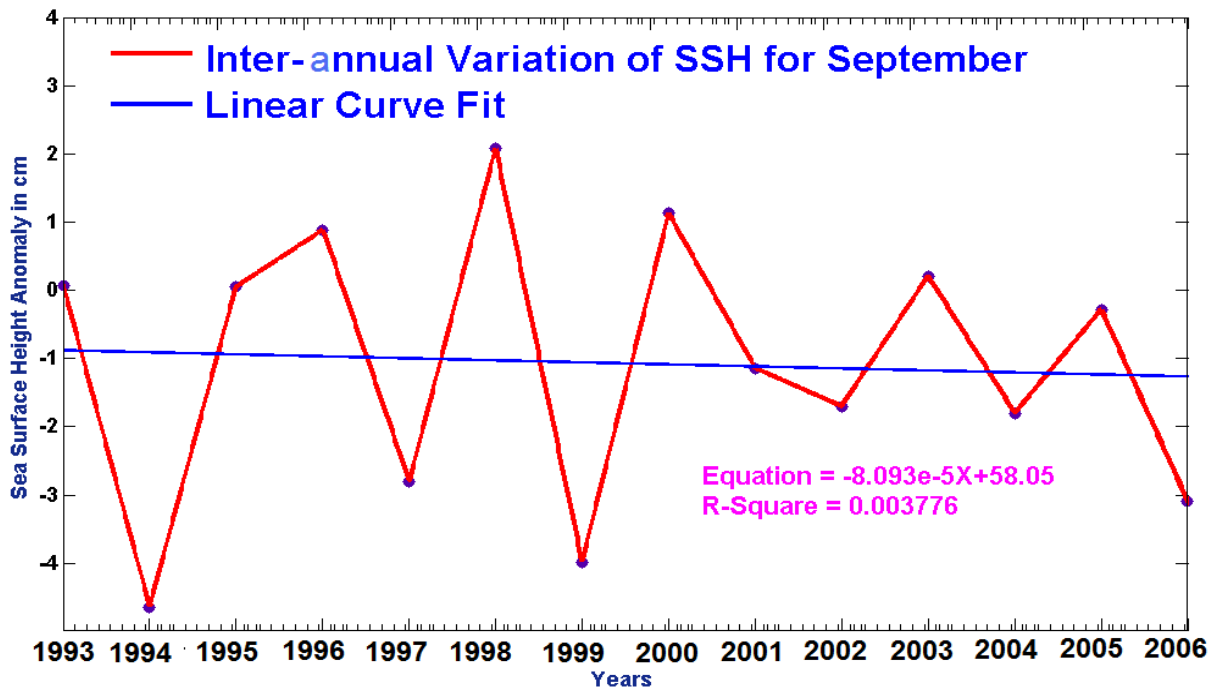


Figure 17 Monthly mean of SSH anomaly for September

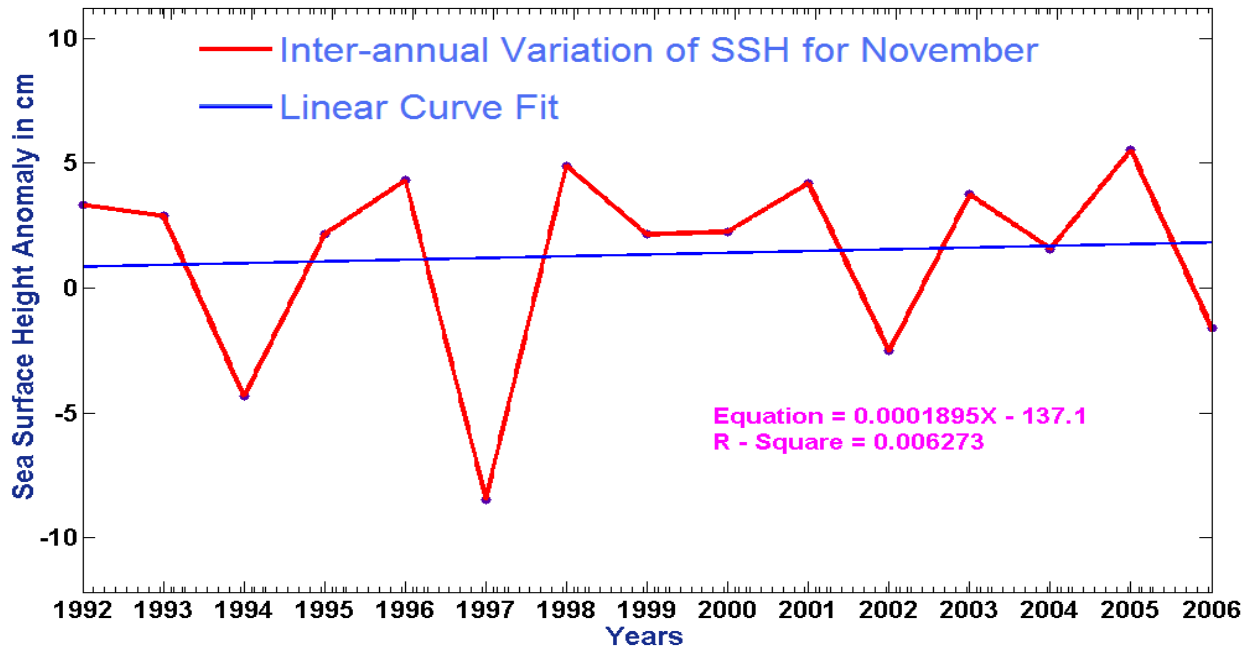


Figure 18 Monthly mean of SSH anomaly for November

From the linear trend line fitted to inter-annual variability of SSH anomaly for the individual month, it is evident that during the month of September (Figure 17) and November (Figure 18) the trend showed a weakly decreasing and weakly increasing trend respectively. In fact, most of the inter-annual variability that we noticed in Figure 14 was contributed by the variability occurring in the month of May and February (Figure 15 & 16).

In summary, the SSH anomaly showed a dominant seasonal signal whose amplitude was about 8cm with maximum sea level occurring during May-June (~4cm) followed by November-December (~1.5cm). The lowest sea level occurred in the month of February (~ -4.5cm) followed by September (~ -1cm). The SSH anomaly showed a large inter-annual variability and the linear trend line showed an increasing sea level anomaly of ~2cm during the period 1992 to 2006.

3.2 Chlorophyll a

Seasonal variability

The monthly mean climatology of Chl-a (Figure 19) showed high Chl-a concentration during July to September with the highest value in August (~0.57mg/m³). The lowest concentration was in the month of April (0.36 mg/m³).

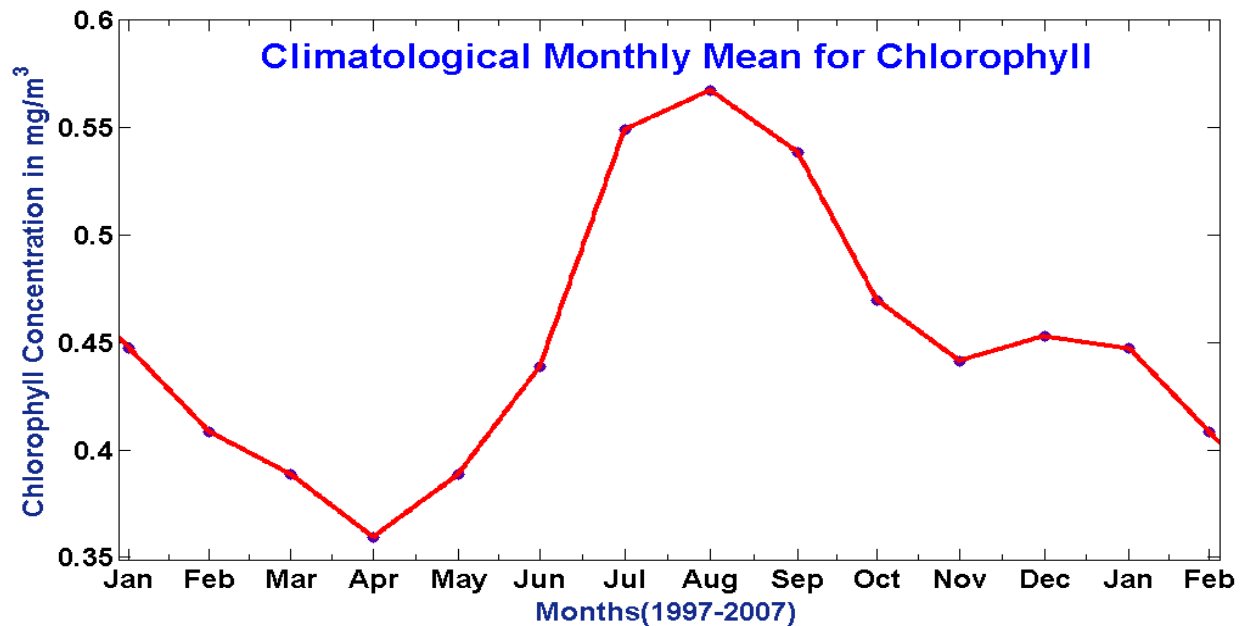


Figure 19 Monthly mean climatology of Chl-a

Inter-annual variability

In order to understand the inter-annual variability, the entire data set was analyzed (Figure 20)

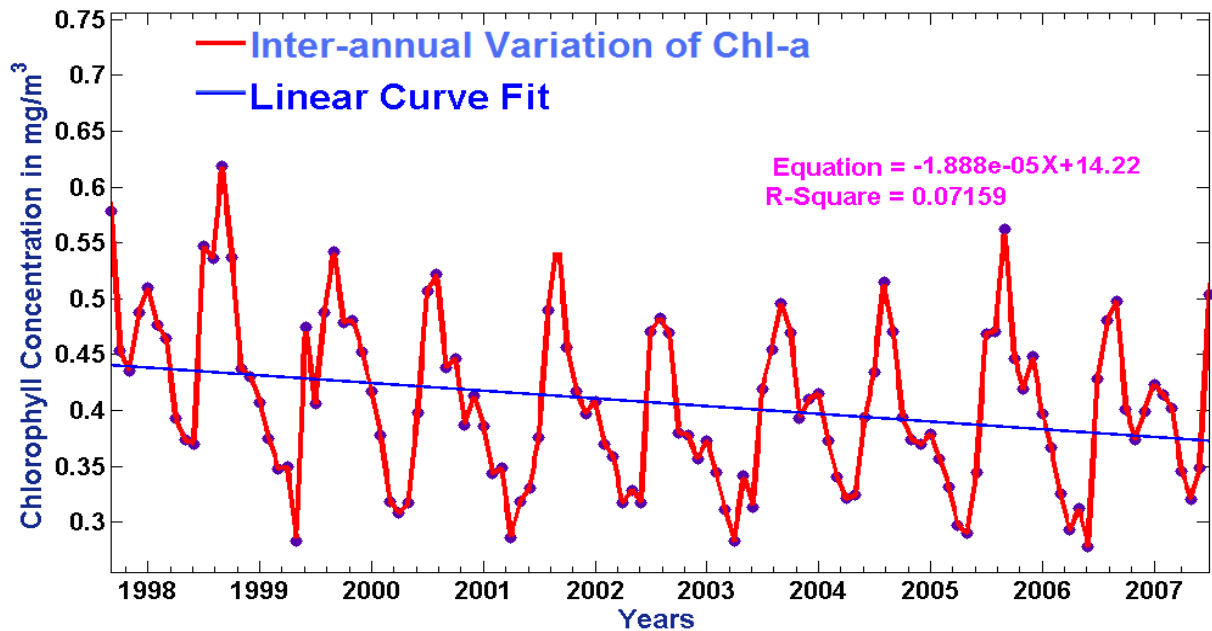


Figure 20 Monthly mean of Chl-a during 1996-2007

The Chl-a curve during 1997 to 2007 consistently showed high chlorophyll concentration occurring in August of every year and the lowest in April, with some amount of inter-annual variability. The linear trend line (solid blue line) fitted to the data showed a marginal decline in the chlorophyll pigment concentration from 0.44mg/m³ to 0.375mg/m³ (Figure 20). Thus, the study showed a net decrease of Chl-a of about 0.08mg/m³ during 1997-2007. As Chl-a showed seasonal variability with maximum in August and minimum in April, we further analyzed the concentration for these 2 months for the study period and presented in Figures 21 and 22.

From the linear trend line fitted to the data, it is evident that both in August and April the variability was almost similar ($\sim 0.04 \text{ mg/m}^3$).

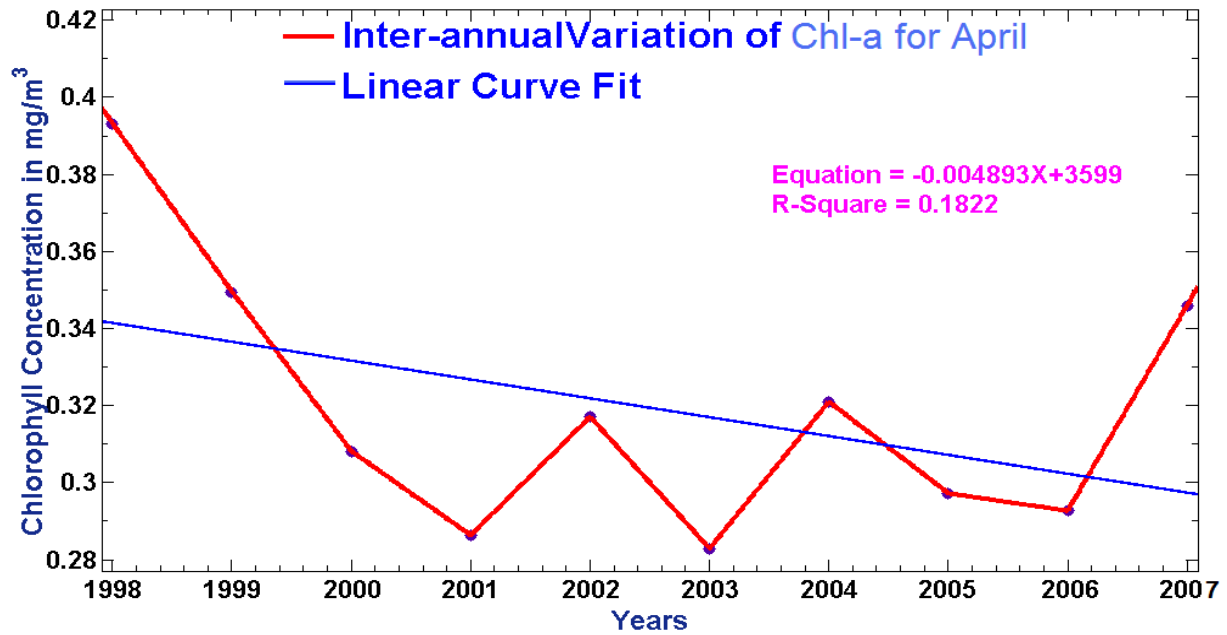


Figure 21 Monthly mean of Chl-a for April

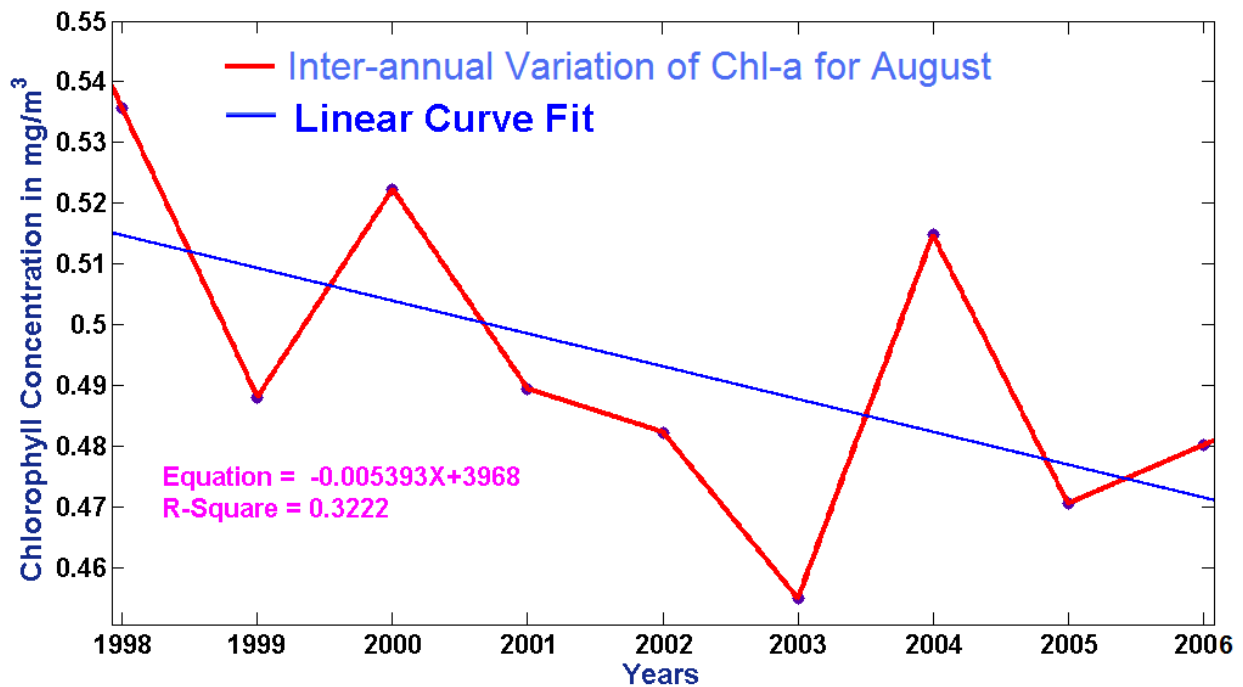


Figure 22 Monthly mean of Chl-a for August

In summary, the chlorophyll pigment concentration showed a dominant seasonal signal with amplitude of about 0.2 mg/m^3 with highest concentrations occurring in August ($\sim 0.57 \text{ mg/m}^3$) and lowest in April ($\sim 0.36 \text{ mg/m}^3$). This seasonality was

observed in the entire data set in a cyclic manner during 1997 to 2007 with some amount of inter-annual variability. The linear trend line showed that during the study period the chlorophyll pigment concentration showed a decrease of about $0.08\text{mg}/\text{m}^3$.

3.3 Photosynthetically Available Radiation

Seasonal variability

The monthly mean climatology of Photosynthetically Available Radiation (PAR) (Figure 23) like the SSH anomaly showed a bi-modal distribution

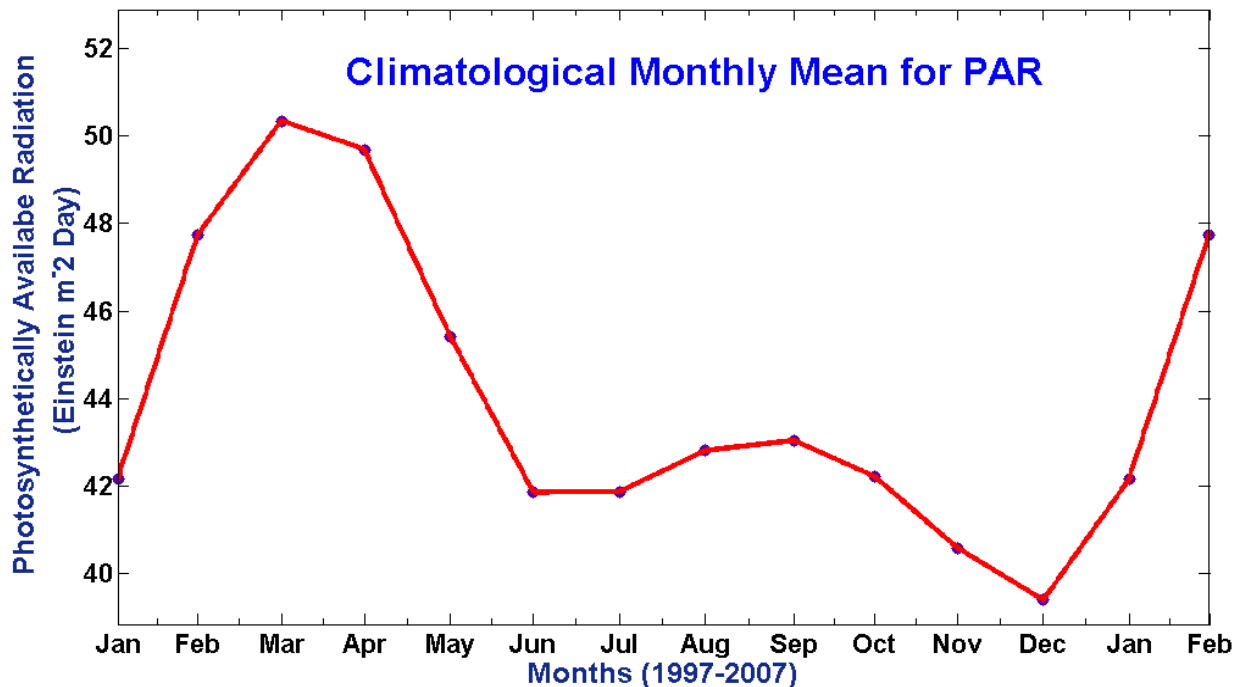


Figure 23 Monthly mean climatology of PAR

Highest value of PAR in March-April (~ 50 Einstein m^{-2} day) followed by a secondary peak in August-September (~ 43 Einstein m^{-2} day). The lowest value of PAR occurred during June-July (~ 42 Einstein m^{-2} day) followed by December (~ 39 Einstein m^{-2} day).

Inter-annual variability

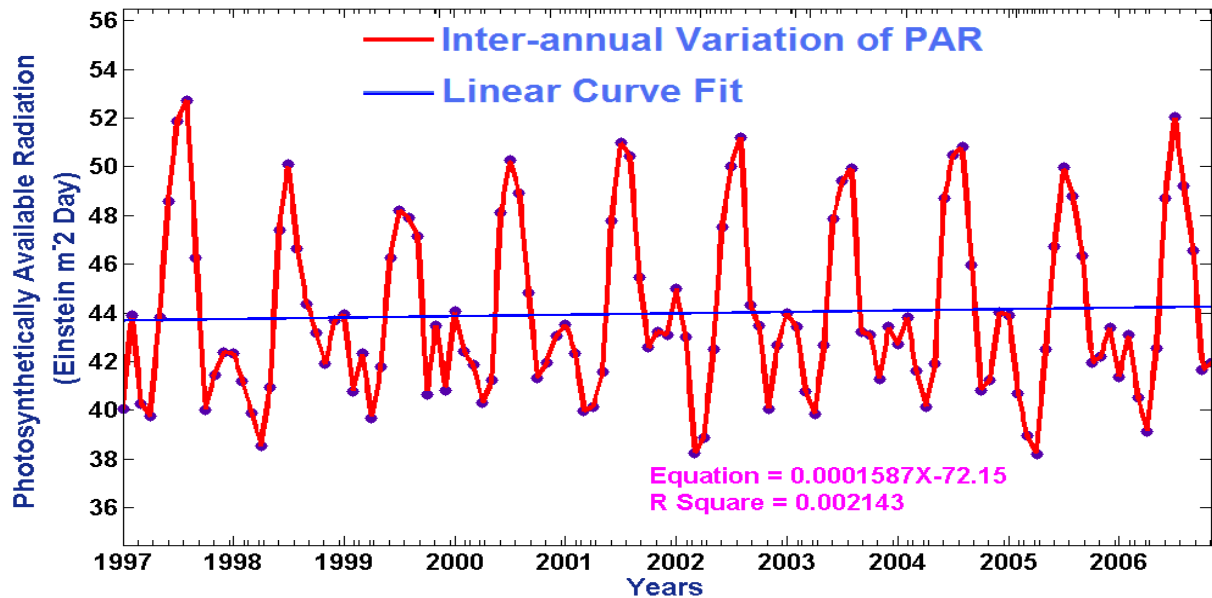


Figure 24 Monthly mean of PAR during (1997-2007)

In order to understand the inter-annual variability, the entire data set was analyzed (Figure 24). The linear trend line did not show any significant trend. Thus, from the data it appears that though there was some inter-annual variability it did not lead to a net increase or decrease.

In summary, PAR also showed a strong seasonality with amplitude of ~10 Einstein m⁻² day with highest value in March and lowest in December. Though the data showed some inter-annual variability, there was no significant trend discernible during the period 1997 to 2007.

3.4 Diffusion Attenuation

Seasonal variability

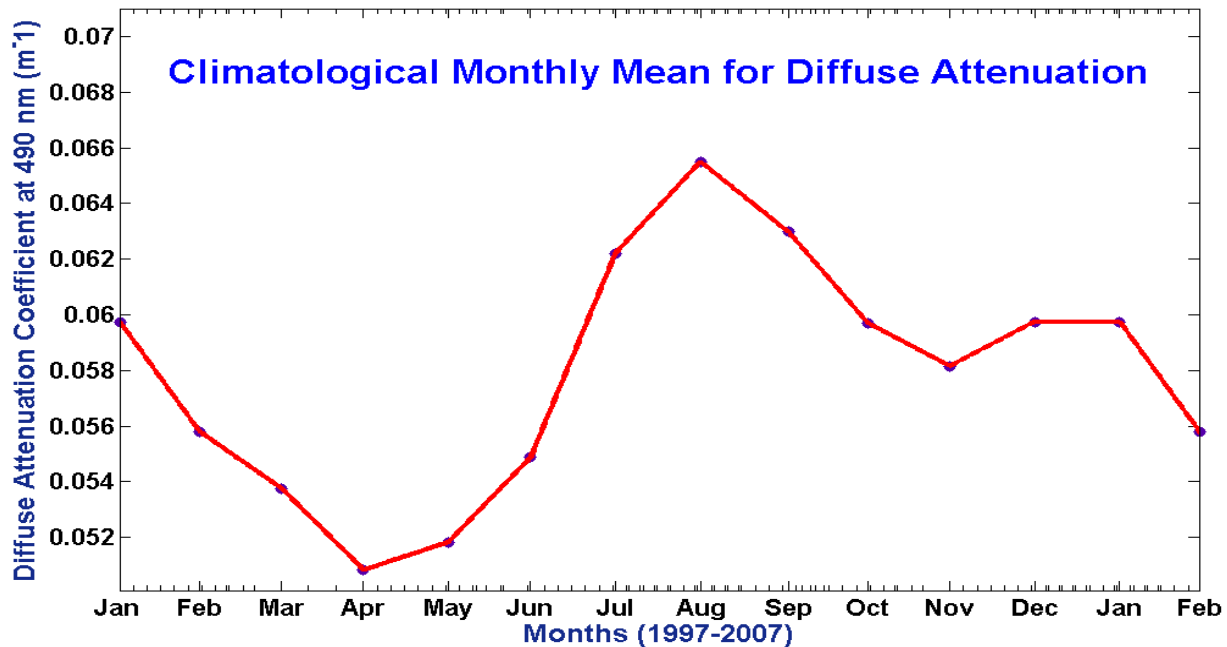


Figure 25 Monthly mean climatology of kd490

The monthly mean climatology of diffuse attenuation (kd490) (Figure 25) showed minimum attenuation in the month of April ($\sim 0.051\text{m}^{-1}$) followed by a peak in August ($\sim 0.066\text{m}^{-1}$).

Inter-annual variability

The Diffusion Attenuation curve varied from 0.058m^{-1} to 0.53m^{-1} (Figure 26). The linear trend line (solid blue line) showed a decreasing trend over the period of study. That is the attenuation decreased with time from 1997 to 2007 to about 0.005m^{-1} which is not a significant variation.

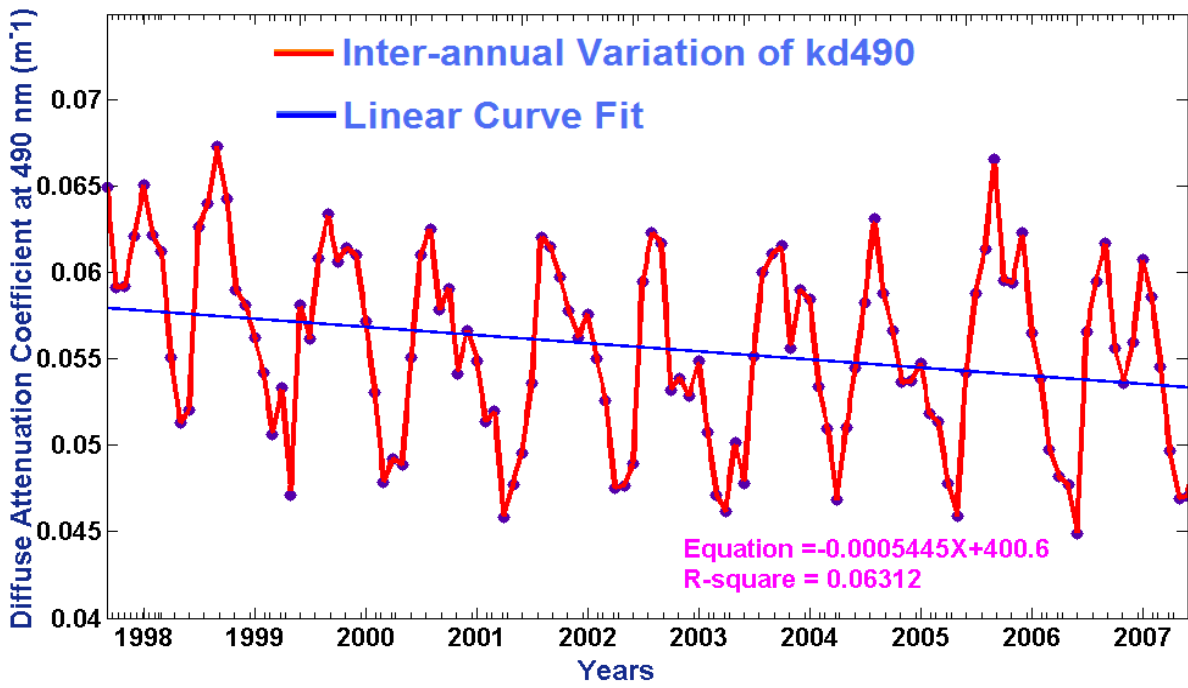


Figure 26 Monthly mean of kd_{490} during (1997-2007)

CHAPTER 3

SUMMARY

Global warming and associated climate change is one of the immediate threats that the human being are confronted with and it is important to understand so that effective remedial measures could be put in place. The response of the earth-ocean-atmosphere system to human-induced climate change varies from region to region and hence studies of regional manifestation forms an important part. Since ocean is a reservoir of CO₂, it is important to understand how oceans are responding to the enhanced warming regime. It is in this context that the present project was conceived which was aimed at understanding how the Bay of Bengal situated in the eastern part of the northern Indian Ocean is responding. The Bay of Bengal was chosen as the study area due to its unique characteristics such as very low salinity waters due to large river runoff, large sediment input from the rivers, occurrence of cyclones, etc. For the present study, to understand how the Bay of Bengal is responding to global warming, we chose to study parameters such as sea level (1992-2006), chlorophyll pigment concentration, photosynthetically available radiation and diffuse attenuation using remote sensing data during the period 1997 to 2007. The sea level changes are directly linked to the global warming, as increased warming will lead to increased sea level rise due to melting of polar ice-caps. The chlorophyll pigment concentration indicates the biological productivity of the region and hence is important to understand its changes. The photosynthetically available radiation (PAR) will determine the quantum of light that is available at the ocean surface while the diffuse attenuation (kd490) determines how much of the light coming to the ocean surface will penetrate downward within the water column. Hence both Par and kd490 is needed to understand the ocean biological productivity.

The SSH anomaly showed a dominant seasonal signal whose amplitude was about 8cm with maximum sea level occurring during May-June (~4cm) followed by November-December (~1.5cm). The lowest sea level occurred in the month of February (~ -4.5cm) followed by September (~ -1cm). The SSH anomaly showed a large inter-annual variability and the linear trend line showed an increasing sea level anomaly of ~2cm during the period 1992 to 2006.

The chlorophyll pigment concentration showed a dominant seasonal signal with amplitude of about 0.2 mg/m^3 with highest concentrations occurring in August ($\sim 0.57 \text{ mg/m}^3$) and lowest in April ($\sim 0.36 \text{ mg/m}^3$). This seasonality was observed in the entire data set in a cyclic manner during 1997 to 2007 with some amount of inter-annual variability. The linear trend line showed that during the study period the chlorophyll pigment concentration showed a decrease of about 0.08 mg/m^3 .

The photosynthetically available radiation also showed a strong seasonality with amplitude of $\sim 10 \text{ Einstein m}^{-2} \text{ day}$ with highest value in March and lowest in December. Though the data showed some inter-annual variability, there was no significant trend discernible during the period 1997 to 2007.

The diffuse attenuation also showed a strong seasonality with minimum attenuation in the month of April ($\sim 0.051 \text{ m}^{-1}$) followed by a peak in August ($\sim 0.066 \text{ m}^{-1}$). Over the study period, diffuse attenuation showed a decreasing trend (about 0.005 m^{-1}).

In summary, the study noted an increasing trend in the sea level (1992-2006) while the chlorophyll pigment concentration showed a decline over the period 1997 to 2007. Though PAR did not show any significant trend, the diffuse attenuation showed a decline, implying that this change is due to the changes in the water column constituents. One of the factors may be the suspended sediment.

References

BOOKS & JOURNALS :

Prasad, T.G., 1997. Annual and seasonal mean buoyancy fluxes for the tropical Indian Ocean. *Current Science* **73**, 667-674.

Subramanian, V., 1993. Sediment load of Indian Rivers, *Current Science* **64**, 928-930.

Levitus, S., Gelfeld, R., Boyer, T., Johnson, D., 1994. Results of the NODC Oceanographic Data Archaeology and Rescue Projects, *Key to Oceanographic Records Documentation* No. **19**, NODC, Washington, D.C., 73pp.

Morel, A., 1980. In-water and remote measurement of ocean color. *Boundary-Layer Meteorology* **18**, 177-201.

Shubha Sathyendranath, 2000. Remote sensing of ocean colour in coastal, and other optically-complex, waters, *IOCCG Report* **3**, Nova Scotia, Canada, 140pp.

WEB SITES :

www.aviso.oceanobs.com/en/altimeter

www.ioccg.org/reports/report3.pdf

<http://www.crisp.nus.edu.sg/~research/tutorial/rsmain.htm>

<http://science.hq.nasa.gov/oceans/living/color.html>

<http://oceancolor.gsfc.nasa.gov>